Jul 1st, 12:00 AM

On-Line Climate Model Simulation of the Global Carbon Cycle and Verification Using the In Situ Observation Data

K. Mabuchi

H. Kida

On-Line Climate Model Simulation of the Global Carbon Cycle and Verification Using the In Situ Observation Data

K. Mabuchi[a] and H. Kida[b]

[a]*Meteorological Research Institute, Japan Meteorological Agency, Nagamine, Tsukuba, Ibaraki 305-0052, Japan*
E-mail: kmabuchi@mri-jma.go.jp

[b]*Department of Geophysics, Graduate school of Science, Kyoto University, Oiwake-cho, Kitashirakawa, Sakyo-ku, Kyoto 606-8502, Japan*

ABSTRACT: Using a global climate model that includes a new land surface ecosystem model, a numerical simulation under conditions of the actual vegetation was performed. The values of atmospheric carbon dioxide concentration calculated by the model were verified using the in situ observation data. Concerning the seasonal cycle patterns in the Northern Hemisphere, the model could successfully reproduce the features of the seasonal cycle patterns of the observed data. Also in the equatorial zone and in the low latitudinal zone in the Southern Hemisphere, the model could generally reproduce the features of the seasonal cycles of the observed data. In the middle and the high latitudinal zones in the Southern Hemisphere, the amplitudes of the seasonal cycles calculated by the model were somewhat larger than those of the observed data. The model could, however, reproduce the typical seasonal cycles in the Southern Hemisphere, which are opposite to those in the Northern Hemisphere. The value of increase trend of the global mean surface carbon dioxide concentration simulated by the model was somewhat larger than that of the observed data. The increase trend should decrease when the effects of the temperature increase and the ocean uptake increase were considered. For the values of carbon cycle elements of all vegetation types mean, although the value of vegetation carbon storage was almost the same as the results of other models, the values of soil carbon storage and net primary production were relatively larger than those of other estimations.

Keywords: Carbon cycle; Ecosystem model; Climate model; Numerical simulation

1. INTRODUCTION

The interaction between land surface vegetation and the atmosphere is a very important element in the Earth's system. With the physical aspects, the climate system and the carbon cycle related to the land surface vegetation are closely interacted. In the past, numerous studies have been performed concerning the land surface process and interactions between the land surface and the atmosphere. The studies of Bounoua et al. [1999] and Mabuchi et al. [2000] focused on vegetation physiology and the carbon circulation associated with vegetation activity and climate. Cao et al. [2005] presented the simulation results of the global scale carbon dioxide exchange between the atmosphere and the terrestrial biosphere in the past long time period using ecosystem models. Kicklighter et al. [1999] and Alexandrov et al. [2003] discussed the effects of carbon dioxide fertilization on the terrestrial carbon budget. Govindasamy et al. [2005] investigated the sensitivity of the feedback between global warming and the carbon cycle for year 2100 global warming scenario using a fully coupled climate and carbon cycle model. Matthews et al. [2005] also examined the behavior of the terrestrial carbon cycle under historical and future climate change using a global climate model coupled to a dynamic terrestrial vegetation and carbon cycle model.

In the present study, for a preceding step of prospective study using a global climate model that includes a new terrestrial ecosystem model, a numerical simulation was performed to verify the global carbon cycle simulated by the model.

2. MODEL DESCRIPTION AND EXPERIMENTAL DESIGN

The atmospheric model used in the experiment is the spectral general circulation model developed by the Japan Meteorological Agency (JMA). This general circulation model has a triangular truncation at wave number 63 (T63), and employs hybrid vertical coordinates at 21 levels. The horizontal resolution is 1.875° (192 × 96 grid points). The basic equations adopted for the model are the primitive equations. The atmospheric

prognostic variables are the temperature, specific humidity, divergence and vorticity of the wind, the carbon dioxide concentration in each atmospheric layer, and surface pressure. The time step interval of the integration is about 20 minutes. The model includes short-wave and long-wave radiation processes. Large scale precipitation and convective precipitation are estimated separately, with convective precipitation calculated by the Kuo scheme [Kuo 1974]. Vertical diffusion is calculated by the turbulent closure model (level 2.0) proposed by Mellor and Yamada [1974].

A Biosphere-Atmosphere Interaction Model Version 2 (BAIM2) was integrated into this general circulation model. The vegetation type at each model grid point was specified and the interactions between the land surface vegetation and the atmosphere were estimated by the BAIM2 at each grid point.

Concerning the terrestrial ecosystem model, a large number of models were already developed. For recent example, Ito and Oikawa [2002], Schwalm and Ek [2004], Garcia-Quijano and Barros [2005], and Matala et al. [2005] presented new ecosystem models. The BAIM2 is also a new terrestrial ecosystem model, and that is an improved land surface model on the basis of the BAIM Version 1 [Mabuchi et al. 1997]. The BAIM2 has two vegetation layers and three soil layers, and predicts the temperature and stored moisture for each layer. The photosynthesis processes for C_3 and C_4 plants are adopted in the model. The carbon storage of vegetation is divided into five components (leaves, trunk, root, litter, and soil), and the carbon exchanges among the components of vegetation and the atmosphere are estimated in each time step of the on-line model integration. The values of a part of the morphological parameters using in the model are derived from the carbon storage values of the components, and the phenological changes of vegetation are reproduced by the model. The model can also predict the ground accumulation and melting of snow, and the freezing and melting of water in the soil.

The vegetation type of each model grid point was fundamentally derived from the Major World Ecosystem Complexes Ranked by Carbon in Live Vegetation data set [Olson et al. 1983]. The actual vegetation of a given global land surface grid was classified into one of 13 types, including the desert and cryosphere. The forest and taiga in East Siberia regarded as needle-leaf deciduous forest type vegetation. In the present experiment, crop type vegetation was regarded as grassland vegetation.

A control time integration was performed. In this control integration, the actual global vegetation and climatic SST values were used. The sea surface temperatures and sea ice values were taken from the GISST2.2 dataset [Rayner et al. 1996]. The monthly climatic values of these data were assigned to each model ocean-area grid point. In order to estimate the initial values of the soil water content, the ice content in the soil, the soil temperature, and the carbon storage of vegetation, a necessary spin-up calculation was carried out. Using the values obtained from the spin-up calculation, the control integration was continued for 10 years.

The initial values of the carbon dioxide concentration in the atmosphere were set to about 360 ppmv. The distribution pattern of the initial values had decreasing gradients toward the upper atmospheric level and toward the South Pole. In the integration, the anthropogenic emission fluxes of the carbon dioxide were taken into account. The value of 0.11 μmol m^{-2} s^{-1} on average for the global land area (about 6.2 GtC $year^{-1}$ for the total of the global land area) was given for the values of those fluxes. The monthly carbon dioxide fluxes between sea surface and the atmosphere were given by the model-calculated data [Obata and Kitamura 2003; Obata, personal communication].

3. VERIFICATION OF THE SIMULATED GLOBAL CARBON CYCLE

The values of the atmospheric carbon dioxide concentration calculated by the model were verified using the in situ observation data in the WMO World Data Centre for Greenhouse Gases (WMO WDCGG) data set that was provided by the Japan Meteorological Agency [JMA 2005].

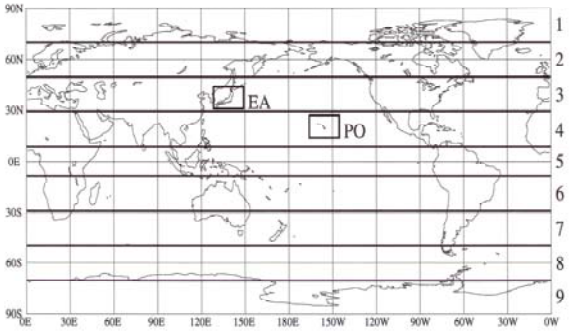

Figure 1. Areas for the verification of the atmospheric carbon dioxide concentration.

Figure 1 indicates the verification areas. Area EA is over the Japanese Islands, and Area PO is over the Hawaiian Islands. These two areas were selected for the typical verification areas to compare directly with the in situ observation stations data. The verifications were also performed for nine latitudinal zones indicated by the numbers on the right hand side of the map.

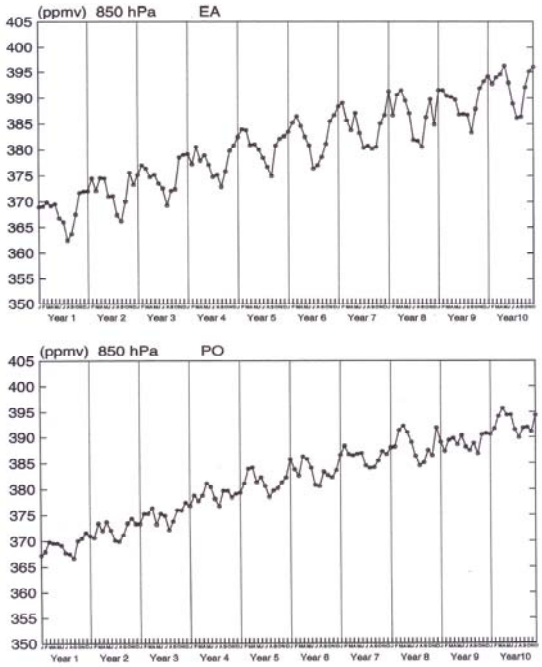

Figure 2. Temporal distributions of the carbon dioxide concentrations (ppmv) calculated by the model. The monthly mean values at the 850-hPa level are indicated. The upper panel indicates the area mean values for Area EA, and lower panel those for Area PO.

Figure 2 indicates the temporal distributions of the carbon dioxide concentrations calculated by the model. The monthly mean values at the 850-hPa level are indicated. The upper panel indicates the area mean values for Area EA, and lower panel those for Area PO. The temporal distributions of the model in Area EA were compared with those of the data observed at the Ryori station in Japan. The typical seasonal change pattern of the carbon dioxide concentration observed at Ryori is as follows (figure is not shown). The amplitude is about from 10 to 15 ppmv. The maximum value appears in April and the minimum value appears in August. The seasonal change pattern of Area EA calculated by the model is generally similar to that at the Ryori station. The temporal distributions of Area PO were compared with those of the observation data at the Mauna Loa station in Hawaii. The typical seasonal change pattern observed at Mauna Loa is as follows (figure is not shown). The amplitude is about 5 ppmv. The maximum value appears in May or June and the minimum value appears in September. Although the seasonal changes reproduced by the model indicated lower panel in Figure 2 are somewhat complicated, the seasonal change pattern of Area PO by the model is generally consistent with that at the Mauna Loa station.

In the WMO WDCGG data set, the data of 81 points in situ observatory (in case of picking up the data from the year 2000 to now) are included. The numbers of observation points those belong in Zone 1 through Zone 9 (Figure 1) are 5, 14, 33, 12, 3, 3, 3, 6, and 2, respectively. The typical seasonal change patterns of the observed carbon dioxide concentration in each zone are as follows (figures are not shown). Concerning the data observed in Zone 1, the amplitude is about 15 ppmv. The maximum value appears in April or May and the minimum value appears in August. In Zone 2, although there are some stations in which the seasonal pattern in the data is not clear, the amplitude is about 15 ppmv or more. The maximum value appears in April and the minimum value appears in August. In Zone 3, the number of observation points (33) belong in this zone is the largest one among the 9 zones. Also in this zone, there are some stations in which the seasonal pattern in the data is not clear. However, the amplitude is typically from about 10 to 15 ppmv, and the maximum value appears in April and the minimum value appears in the month from July to September. In Zone 4, the amplitude is about 5 ppmv, and the maximum value appears in April or May and the minimum value appears generally in September. In Zone 5, which covers over the equatorial area, the amplitude is about 3 ppmv. In this zone, the months, in which the maximum and the minimum values appear, are changed, depend on the location of the observatory. In Zone 6, although the seasonal cycle pattern is not clear, the amplitude is less than 3 ppmv. In Zones 7, 8, and 9, the amplitudes are generally less than 3 ppmv. Although the amplitudes are small, there are clear seasonal cycle patterns. The maximum value appears in September or October and the minimum value appears in March or around months. These seasonal cycle patterns are opposite to those in the Northern Hemisphere zones.

Figure 3 indicates the temporal distributions of the zonal mean values of the monthly mean carbon dioxide concentrations calculated by the model. In the Northern Hemisphere (Zones 1, 2, 3, and 4), the model can successfully reproduce the features of the seasonal cycle patterns of the observed data described above. Also in Zones 5 and 6, the model can generally reproduce the features of the seasonal cycles of the observed data. Especially in Zone 5, there is a clear seasonal pattern that is two cycles per year. This seasonal pattern of the model appears in Zone 5 is due to the effect of the opposite seasonal cycles between in the Northern Hemisphere and in the Southern Hemisphere. In Zones 7, 8, and 9, the amplitudes of the seasonal cycles simulated by the model are somewhat larger than those of the observed data, in particular in Zones 8 and 9. The model can, however, reproduce the typical seasonal cycles in the Southern Hemisphere, which are opposite to those in the Northern Hemisphere.

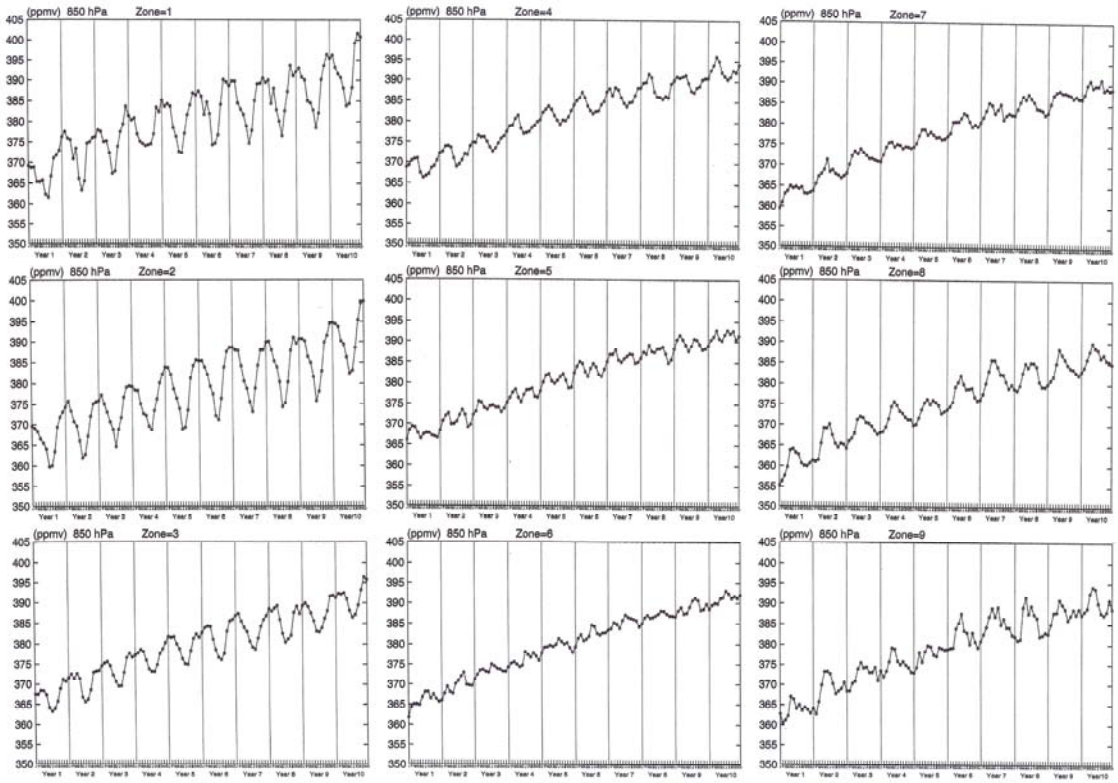

Figure 3. The same as in Figure 2, except for the zonal mean values from Zone 1 to 9. In the left hand side column, the upper panel indicates the values in Zone 1, the middle those in Zone 2, and the bottom those in Zone 3. In the central column, the upper panel indicates the values in Zone 4, the middle those in Zone 5, and the bottom those in Zone 6. In the right hand side column, the upper panel indicates the values in Zone 7, the middle those in Zone 8, and the bottom those in Zone 9.

Table 1 indicates the mean values of carbon budget for the main vegetation types (10 types) and for all vegetation types mean at the 10-year period simulated by the model. In Table 1, the values of soil carbon storage (SC) of Types 6 (C_3 grass land), 14 (mixed forest), and 15 (needle leaf evergreen forest) become relatively large values, compared with those of the vegetation types located in the warm climate regions. In this model, the value of soil carbon storage of Type 17 (polar tundra) becomes small value due to the small biomass value in the polar region. The values of GPP and NPP of Type 12 (tropical rain forest) and Type 18 (C_4 grass land) are relatively large values caused by the high vegetation activities in the warm climate regions. For the values of each element of all vegetation types mean (Global), the vegetation carbon storage (VC) is 677.4 PgC, the soil carbon storage (SC) is 1,852.2 PgC, the gross primary production (GPP) is 158.7 PgC/year, the net primary production (NPP) is 91.2 PgC/year, and the net ecosystem production (NEP) is 3.9 PgC/year. In these model results, although the value of VC is almost the same as the results of other models, the values of SC and NPP are relatively larger than those of other estimations.

Table 1. The mean values of carbon budget for the main vegetation types at the 10-year period simulated by the model. VC: vegetation carbon (KgC m $^{-2}$), SC: soil carbon (KgC m $^{-2}$), GPP: gross primary production (gC m $^{-2}$ year $^{-1}$), LTR: litter flux (gC m $^{-2}$ year $^{-1}$), RRV: respiration from vegetation (gC m $^{-2}$ year $^{-1}$), RRS: respiration from soil (gC m $^{-2}$ year $^{-1}$), NPP: net primary production (gC m $^{-2}$ year $^{-1}$), NEP: net ecosystem production (gC m $^{-2}$ year $^{-1}$). Type 6 indicates the C_3 grass land type, Type 10 is the tropical seasonal forest, Type 12 is the tropical rain forest, Type 13 is the broadleaf deciduous forest, Type 14 is the mixed forest, Type 15 is the needle leaf evergreen forest, Type 16 is the needle leaf deciduous forest, Type 17 is the polar tundra, Type 18 is the C_4 grass land (including the savanna type vegetation), Type 19 is the arid semi desert, and Global is all vegetation types mean. Numbers in parentheses are grid point numbers for each vegetation type.

Type	6 (613)	10 (315)	12 (136)	13 (125)
VC	1.39	7.91	18.94	8.70
SC	25.53	11.45	11.12	14.44

GPP	1213.5	1329.6	3737.2	1291.1
LTR	853.4	689.5	1795.3	676.1
RRV	354.2	626.5	1924.7	596.8
RRS	806.0	705.6	1761.3	699.3
NPP	859.4	703.1	1812.5	694.3
NEP	53.3	- 2.5	51.2	- 5.0
Type	14 (51)	15 (663)	16 (258)	17 (445)
VC	8.59	9.99	1.96	0.11
SC	32.90	29.54	16.36	3.23
GPP	1575.9	1445.2	524.1	52.3
LTR	1072.6	861.3	449.5	46.0
RRV	477.3	568.9	73.5	6.0
RRS	987.0	786.4	415.4	51.5
NPP	1098.7	876.3	450.6	46.3
NEP	111.7	90.0	35.3	- 5.3
Type	18 (434)	19 (629)		Global
VC	1.44	0.09		4.55
SC	11.95	5.22		12.44
GPP	2443.7	244.7		1065.9
LTR	1212.7	200.1		604.3
RRV	1225.8	44.9		453.7
RRS	1225.9	187.0		586.6
NPP	1217.9	199.8		612.6
NEP	- 8.0	12.8		26.1

4. DISCUSSIONS

Using a global climate model that includes a new land surface ecosystem model BAIM2, a numerical simulation under conditions of the actual vegetation was performed. The values of atmospheric carbon dioxide concentration calculated by the model were verified using the in situ observation data in the WMO WDCGG data set.

The value of increase trend of the global mean surface carbon dioxide concentration simulated by the model in the 10-year period control run was 2.8 ppmv year $^{-1}$. This trend value is somewhat larger than that of the observed data. In this model simulation, the effects of the temperature increase by the global warming were not considered. Although the effects of the increase of carbon dioxide uptake by the land surface vegetation due to the effect of carbon dioxide fertilization were reproduced, the effects of the increase of carbon dioxide uptake by the ocean due to the increase of the carbon dioxide concentration in the atmosphere were also not considered. The increased trend of carbon dioxide concentration in the model atmosphere should change when the effects of the temperature increase and the increase in ocean uptake are considered.

In the middle and the high latitudinal zones in the Southern Hemisphere, the amplitudes of the seasonal cycles of carbon dioxide concentration simulated by the model were larger than those of the observed data. In the model, there is a possibility that the effects of seasonal change of the vegetation activity in the mid-latitude in the Southern Hemisphere are greater than those of the actual.

Concerning the global carbon budget simulated by the model, the value of soil carbon storage was relatively larger than those of other estimations. The soil carbon storage values estimated by the plot scale investigations are about 1,730 PgC on average [Ito 2002]. Other representative values are 1,567 PgC [IGBP-DIS 2000], and 1,500 PgC [IPCC 2001]. However, the soil carbon storage values that have been estimated have wide range values. Furthermore, these values are generally those in the soil layer near the surface. Therefore, it is considered that the value of 1,852.2 PgC estimated in this model is in the range of the actual values.

The global mean net primary production simulated by this model was relatively larger than those of other model results. The value of NPP is generally a half of the value of GPP. In this model results, the NPP values in the cold climate regions became generally larger than half values of GPP. There is a possibility that the estimated values of respiration from vegetation for the vegetations in the cold regions were too small, and the values of NPP for those vegetations estimated by this model became relatively large values.

The results of the numerical simulation describe above was generally consistent with observed data. There were, however, some discrepancies in the model results. There is a necessity of the further verification using the observation data that can be obtained.

5. ACKNOWLEDGEMENTS

The authors wish to express their thanks to Dr. Akihiko Ito of the Frontier Research System for Global Change, Dr. Georgii Alexandrov of the National Institute for Environmental Studies, and Prof. Takehisa Oikawa of the University of Tsukuba, for many helpful suggestions and discussion. Special thanks are extended to Prof. Tetsuzo Yasunari of Nagoya University, Prof. Masahiro Amano of Waseda University, and Prof. Tatsuo Sweda of Ehime University, for helpful suggestions. Reviewers provided helpful comments for improving the quality of this paper. This research was partially supported by the Global environment research Fund of the Ministry of the Environment and also supported by the Grants-in-Aid for Scientific Research #14208062 of the Ministry of Education, Culture, Sports, Science and Technology. The model computations were performed on the

NEC SX-6 super computers.

6. REFERENCES

Alexandrov, G. A., T. Oikawa, and Y. Yamagata, Climate dependence of the CO_2 fertilization effect on terrestrial net primary production, *Tellus*, 55B(2), 669-675, 2003.

Bounoua, L., G. J. Collatz, P. J. Sellers, D. A. Randall, D. A. Dazlich, S.O. Los, J. A. Berry, I. Fung, C. J. Tucker, C. B. Field, and T. G. Jensen, Interactions between vegetation and climate: Radiative and physiological effects of doubled atmospheric CO_2, *Journal of Climate*, 12, 309-324, 1999.

Cao, M., S. D. Prince, B. Tao, J. Small, and K. Li, Regional pattern and interannual variations in global terrestrial carbon uptake in response to changes in climate and atmospheric CO_2, *Tellus*, 57B(3), 210-217, 2005.

Garcia-Quijano, J. F., and A. P. Barros, Incorporating canopy physiology into a hydrological model: photosynthesis, dynamic respiration, and stomatal sensitivity, *Ecological Modelling*, 185, 29-49, 2005.

Govindasamy, B., S. Thompson, A. Mirin, M. Wickett, K. Caldeira, and C. Delire, Increase of carbon cycle feedback with climate sensitivity: results from a coupled climate and carbon cycle model, *Tellus*, 57B(2), 153-163, 2005.

IGBP-DIS (International Geosphere-Biosphere Program, Data and Information Services), *Global Soil Data Products CD-ROM*, Oak Ridge National Laboratory, Oak Ridge, 2000.

IPCC (Intergovernmental Panel on Climate Change), *Climate Change 2001: the Scientific Basis*, 881pp, Cambridge University Press, Cambridge, 2001.

Ito, A., Soil organic carbon storage as a function of the terrestrial ecosystem with respect to the global carbon cycle, *Japanese Journal of Ecology*, 52, 189-227, 2002 (in Japanese).

Ito, A., and T. Oikawa, A simulation model of the carbon cycle in land ecosystems (Sim-CYCLE): a description based on dry-matter production theory and plot-scale validation, *Ecological Modelling*, 151, 143-176, 2002.

JMA (Japan Meteorological Agency), *WMO World Data Centre for Greenhouse Gases data set*, WMO WDCGG, Tokyo, 2005.

Kicklighter, D. W., M. Bruno, S. Dönges, G. Esser, M. Heimann, J. Helfrich, F. Ift, F. Joos, J. Kaduk, G. H. Kohlmaier, A. D. McGuire, J. M. Melillo, R. Meyer, B. Moore III, A. Nadler, I. C. Prentice, W. Sauf, A. L. Schloss, S. Sitch, U. Wittenberg, and G. Würth, A first-order analysis of the potential rôle of CO_2 fertilization to affect the global carbon budget: a comparison of four terrestrial biosphere models, *Tellus*, 51B(2), 343-366, 1999.

Kuo, H. L., Further studies of the influence of cumulus convection on large scale flow, *Journal of Atmospheric Sciences*, 31, 1232-1240, 1974.

Mabuchi, K., Y. Sato, H. Kida, N. Saigusa, and T. Oikawa, A Biosphere – Atmosphere Interaction Model (BAIM) and its primary verifications using grassland data, *Papers in Meteorology and Geophysics*, 47(3/4), 115-140, 1997.

Mabuchi, K., Y. Sato, and H. Kida, Numerical study of the relationships between climate and the carbon dioxide cycle on a regional scale, *Journal of the Meteorological Society of Japan*, 78(1), 25-46, 2000.

Matala, J., R. Ojansuu, H. Peltola, R. Sievänen, and S. Kellomäki, Introducing effects of temperature and CO_2 elevation on tree growth into a statistical growth and yield model, *Ecological Modelling*, 181, 173-190, 2005.

Matthews, H. D., A. J. Weaver, and K. J. Meissner, Terrestrial carbon cycle dynamics under recent and future climate change, *Journal of Climate*, 18, 1609-1628, 2005.

Mellor, G. L., and T. Yamada, A hierarchy of turbulent closure models for planetary boundary layers, *Journal of Atmospheric Sciences*, 31, 1791-1806, 1974.

Obata, A., and Y. Kitamura, Interannual variability of the sea-air exchange of CO_2 from 1961 to 1998 simulated with a global ocean circulation- biogeochemistry model, *Journal of Geophysical Research*, 108(C11), 3337, doi:10.1029/2001JC001088, 2003.

Olson, J. S., J. A. Watts, and L. J. Allison, *Carbon in Live Vegetation of Major World Ecosystems, ORNL-5862, Environmental Sciences Division Publication No. 1997*, Oak Ridge National Laboratory, Oak Ridge, Tennessee, 1983.

Rayner, N. A., E. B. Horton, D. E. Parker, C. K. Folland, and R. B. Hackett, *Version 2.2 of the Global Sea-Ice and Sea Surface Temperature data set, 1903-1994. CRTN 74*, Hadley Centre for Climate Prediction and Research, Meteorological Office, London Road, Bracknell, Berkshire, RG12 2SY, 1996.

Schwalm, C. R., and A. R. Ek, A process-based model of forest ecosystems driven by meteorology, *Ecological Modelling*, 179, 317-348, 2004.